



# Patterns of density dependence in measles dynamics

Bärbel Finkenstädt, Matthew Keeling and Bryan Grenfell

Department of Zoology, University of Cambridge, Cambridge CB2 3EJ, UK

An important question in metapopulation dynamics is the influence of external perturbations on the population's long-term dynamic behaviour. In this paper we address the question of how spatiotemporal variations in demographic parameters affect the dynamics of measles populations in England and Wales. Specifically, we use nonparametric statistical methods to analyse how birth rate and population size modulate the negative density dependence between successive epidemics as well as their periodicity. For the observed spatiotemporal data from 60 cities, and for simulated model data, the demographic variables act as bifurcation parameters on the joint density of the trade-off between successive epidemics. For increasing population size, a transition occurs from an irregular unpredictable pattern in small communities towards a regular, predictable endemic pattern in large places. Variations in the birth rate parameter lead to a bifurcation from annual towards biennial cyclicity in both observed data and model data.

**Keywords:** measles metapopulation; cyclicity in measles epidemic time-series; nonparametric density estimation; nonlinear demographic dynamics; bifurcation

## 1. INTRODUCTION

The search for pattern in population ecology has benefited enormously from the insights provided by simple deterministic models (May 1982). The main dynamical object here is the *attractor*, which summarizes the model population's long-term dynamics. The most obvious questions about the attractor are its nature (stable equilibrium point, limit cycle, chaos) and its possible coexistence with other attractors. We are also often interested in the behaviour of the system when extrinsic perturbations throw it off the attractor. The latter process lies at the heart of the debate about the impact of environmental noise on intrinsic density-dependent population processes (Rand & Wilson 1991; Bjørnstad *et al.* 1995, 1996; Hill *et al.* 1996; Sutcliffe *et al.* 1996, 1997; Ranta *et al.* 1997). In small populations—or small components of large ones—the deterministic clockwork is also potentially complicated by the vagaries of individual behaviour. In practice, the influence of this demographic noise has been particularly studied in ecological metapopulations—with small spatially coupled units (Gilpin & Hanski 1991)—and in the persistence of epidemics in small populations (Bartlett 1956, 1957, 1960).

In parallel with these theoretical developments, statistical studies of population time-series have addressed similar issues. They have focused in particular on evidence for cycles and other recurrent population behaviour (Royama 1992; Bjørnstad *et al.* 1995, 1996; Costantino *et al.* 1995, 1997; Stenseth *et al.* 1996*b*), the density-dependent forces that generate them (Stenseth *et al.* 1996*a*; Framstad *et al.* 1997; Saitoh *et al.* 1997), and the impact of external perturbations on this picture (Higgins *et al.* 1997). In order to explore all these effects fully, we ideally require a system both replete with high-quality population data and

simple enough to make relatively accurate models. Such populations are rare in ecology.

One example—rarely exploited in an ecological context—is provided by the great microparasitic diseases of childhood (Bartlett 1956, 1957, 1960; Schenzle 1984; Dietz & Schenzle 1985; Schaffer & Kot 1985; Olsen *et al.* 1988; Anderson & May 1991; Nee 1994; Bolker & Grenfell 1995; Grenfell *et al.* 1995*b*; Keeling & Grenfell 1997). The paradigm here is measles, where widespread disease notification schemes, coupled with a relatively simple natural history, have led to a mass of spatiotemporal incidence data and a family of relatively realistic models. Over the last decade, these characteristics have attracted considerable attention from population dynamicists in search of chaos and coexisting attractors (Schenzle 1984; Schaffer & Kot 1985; Olsen *et al.* 1988; Rand & Wilson 1991). However, the specific ecological question of how the measles attractor is affected by demographic and environmental perturbations has not been studied. Addressing this question is the aim of the present study, where we focus on the dynamics of measles in England and Wales.

Measles epidemics essentially reflect a predator–prey interaction between infected and susceptible individuals (Anderson & May 1991). The infectious period, of around a week, is followed by prolonged immunity. Major epidemics are therefore self-limiting. Due to the depletion of susceptibles, subsequent epidemics can occur only after susceptible densities are topped up by births. In England and Wales before vaccination, this pattern led to a regular biennial sequence of epidemics (figure 1*a*), especially in cities large enough to maintain a chain of transmission in epidemic troughs.

The key quantity here is the critical community size (CCS) of about 250 000 inhabitants (Bartlett 1957, 1960), which is the population size large enough to maintain

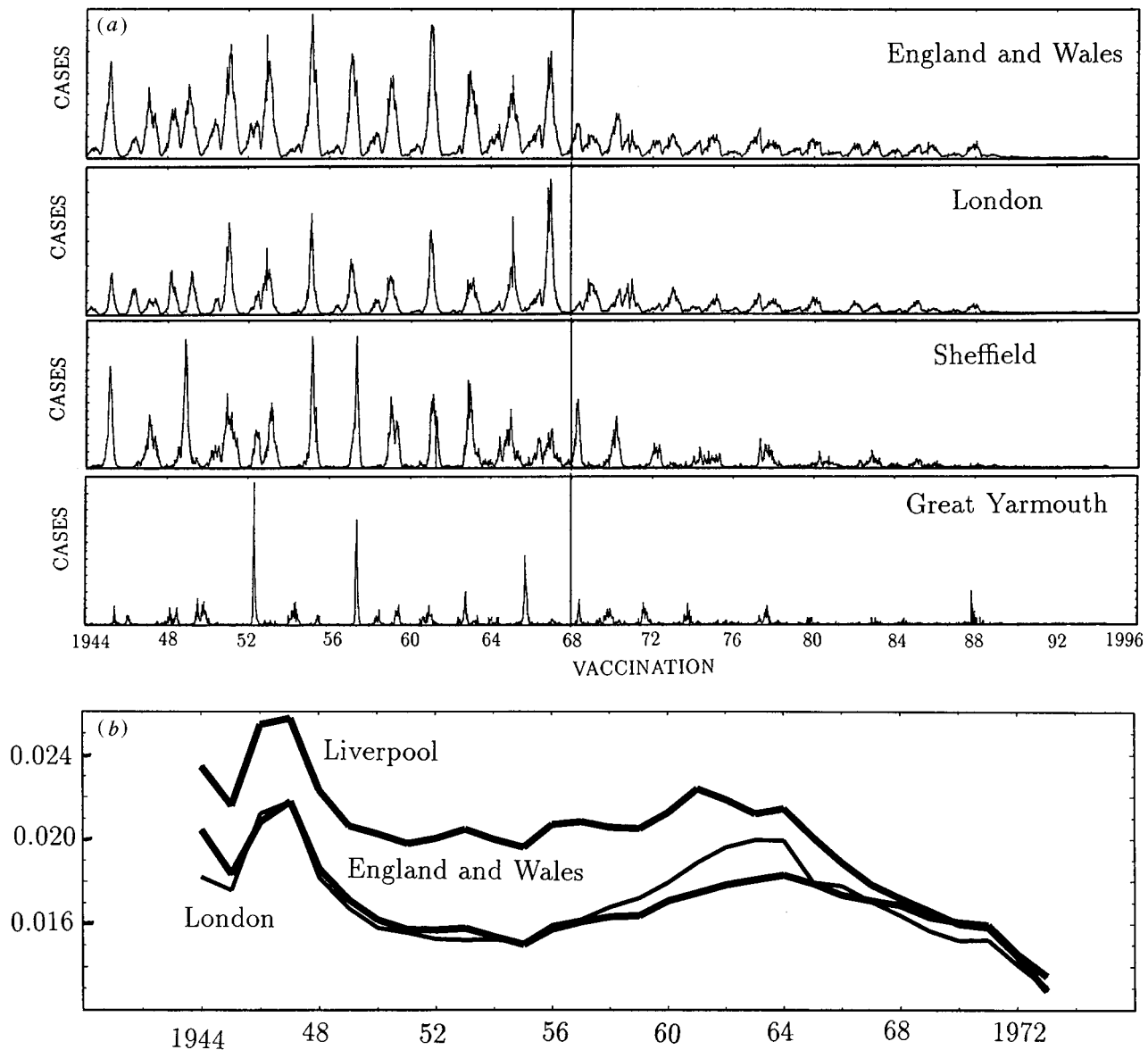


Figure 1. (a) Time-series plot of the measles notifications for the aggregate 60 cities in England and Wales: London (3.3 million inhabitants), Sheffield (500 000 inhabitants), Great Yarmouth (50 000 inhabitants) from 1944 to 1994 (cases are re-scaled for comparison). The vaccination programmes started in 1968. (b) Yearly birth rates (births per capita) for Liverpool, London, England and Wales (average over 60 cities) from 1944 to 1973.

transmission in epidemic troughs. Bartlett (1957) categorized the regular biennial dynamics generally observed in large centres above the CCS as type I behaviour. In smaller centres below the CCS he distinguished regular biennial epidemics with fadeouts in the intervening troughs (type II) from irregular (type III) patterns in small centres, especially when the latter are geographically isolated (Grenfell 1992; Rhodes *et al.* 1997). Type III epidemics are characterized by long periods of extinction of epidemics in the troughs between epidemics ended by reintroduction of infection from other areas.

We explore two aspects of the behaviour of the measles attractor.

#### (a) *Patterns of density dependence*

In a previous publication (Finkenstädt & Grenfell 1998), we used a generalized linear model (GLM) approach to quantify the relative influence of birth rate and population

size variation on the total number of cases. We showed that the number of cases in successive biennial cycles is proportional to the population size, allowing for changes in recruitment of susceptibles due to temporal birth rate variations. In terms of our search for the behaviour of the measles attractor, this implies a negative density dependence between the height of successive major and minor epidemics. We explore this below, using both measles time-series data and the output of compartment models for infectious dynamics. The analysis of observed and model time-series is based on nonparametric density estimation (Silverman 1986).

#### (b) *Impact of birth rate variations*

An especially powerful test of our understanding of population dynamics is provided by exploring how changes in population parameters affect the system's attractor. Recent ecological studies have adopted this

approach to considerable effect, using a combination of models and data analysis. In an experimental flour beetle (*Tribolium*) system, Costantino and co-workers (Dennis *et al.* 1995; Costantino *et al.* 1995, 1997) modified demographic parameters to induce bifurcations predicted by models. Similarly, observed latitudinal gradients in small mammal dynamics appear to be driven by observed parameter variations (Bjørnstad *et al.* 1995; Stenseth *et al.* 1996b).

For measles in the UK, the major demographic variation over the last 50 years has been a modulation in the spatiotemporal pattern of recruitment of susceptibles. These changes were driven by spatial and temporal birth rate variations and by the onset of mass vaccination. In general, the impact of increases in birth rate on the dynamics of measles models is well understood. The most dramatic effect is observed in developing countries, where high birth rates generate annual epidemics (McClean & Anderson 1988a,b), in contrast to the generally biennial pattern seen in developed countries (figure 1a). Simple models for the nonlinear dynamics of seasonally forced epidemics also reflect this transition with increasing birth rate, from longer period (biennial or chaotic) patterns to annual epidemics (Grenfell *et al.* 1994a).

The observed measles data set for England and Wales shows a very similar relationship between birth rates and the pattern of epidemics (Grenfell *et al.* 1995a). In our previous paper (Finkenstädt & Grenfell 1998), we show that birth rates influence the dynamics of measles especially strongly in the troughs between epidemics.

Birth rate variations affect the recruitment rate of new susceptibles. Figure 1b shows that the observed birth rate is subject to variations in both space and time. For instance, Liverpool generally had a higher birth rate than London. However, temporal variations can be observed as well—in particular, for British cities, the birth rate series has a distinct peak around 1947. In this paper, we tease out how birth rate and population size affect the observed dynamics of the epidemics, and draw a comparison with equivalent model predictions.

The other major variation in the susceptible recruitment rate over the last 50 years has been the introduction of mass vaccination in 1968. We therefore finally assess how vaccination affected the density-dependent signature in successive epidemics. Vaccination effectively reduces the recruitment rate of susceptible children. Vaccine uptake stayed at around 60% until the late 1980s when it increased to around 90% (Grenfell & Harwood 1997).

## 2. DATA SETS AND METHODS

### (a) Data

#### (ii) Observed data

We focus on weekly measles notifications in 60 towns and cities in England and Wales. These are official notifications, taken from the Registrar General's Weekly Reports—more details of the data set are given by Keeling & Grenfell (1997). We analyse data from two eras:

1. *Pre-vaccination* recorded cases from 1948 to 1966. These cover nine biennial waves for each town.
2. *Post-vaccination* recorded cases from 1972 to 1994. These cover 11 biennial intervals.

The counts are corrected for a 60% underreporting rate throughout both periods (Clarkson & Fine 1985). Furthermore, local annual birth rates and population sizes are taken from the Annual Reports of the Registrar General. Finkenstädt & Grenfell (1998) found that the four-year lag in birth rate—reflecting the delay before recruitment of school susceptibles—provided the best explanatory variable for the measles trough behaviour. We therefore chose this lag length in the following analyses.

#### (ii) Model data

The model data were obtained from stochastic simulations of an age structured model (the pulsed realistic age-structured (PRAS) model) for measles (Keeling & Grenfell 1997). We use 300-year samples, after 50 years have been discarded to remove transient phenomena. For all simulations the birth rate and death rate were assumed to be equal, so that the total population size displays only small stochastic fluctuations about a constant value. For comparison with observed epidemic dynamics the three population sizes simulated were 20 000, 200 000 (just below the CCS) and 2 million. The results were also obtained for three levels of birth rates: low (0.015 per person per year), medium (0.02), and high (0.024). Finally, to prevent extinction of the disease, a low immigration rate of infectious individuals was included. Following Olson *et al.* (1988), we used a mean importation rate of 20 individuals per million population size. Recent work by us, based on Bartlett's (1956) classic study of the spatial dynamics of measles, indicates that we can scale the level of importation as the square root of population size. We therefore use the formula

$$\text{average number of imports per year} = 0.02\sqrt{\text{population size}}.$$

Finally, to simulate imports coming from the surrounding towns and cities more accurately, the rate of import was taken as being proportional to the number of cases on the biennial attractor of the deterministic system. We stress that the following model results are not qualitatively sensitive to the assumed pattern of imports (Keeling & Grenfell 1998).

### (b) Statistical methods

As in the previous analysis, we distinguish between the *major* and *minor* epidemic year of each biennial wave. Here, a 'year' is defined as the time from the beginning of October to the end of September, and so each year captures a full minor or major epidemic wave. Typically, the major epidemic years cover the peaks in the time-series, whereas the minor epidemic years coincide with the minor outbreaks during the intervening trough time (figure 1a).

For each city, weekly cases are summed over the year and then divided by the contemporaneous population size. This gives a series  $c_{i,t}$  of standardized proportions of cases for community  $i$  ( $i = 1, \dots, 60$ ) in year  $t$  where  $t = 1948, \dots, 1966$  for the pre-vaccination era and  $t = 1972, \dots, 1994$  for the post-vaccination era. The same procedure is applied to the model simulations. Since the number of cases is proportional to the population size (Finkenstädt & Grenfell 1998), the standardized counts,  $c_{i,t}$ , have comparable ranges for different cities,  $i$ .

The behaviour of the time-series  $c_{i,t}$  is analysed throughout the paper by a set of three plots:

1. The scatterplot as a delay plot of  $c_{i,t}$  against  $c_{i,t-1}$ .
2. A surface showing the joint density of the scatterpoints, estimated via nonparametric kernel smoothing (Silverman 1986), where we chose the two-dimensional Gaussian

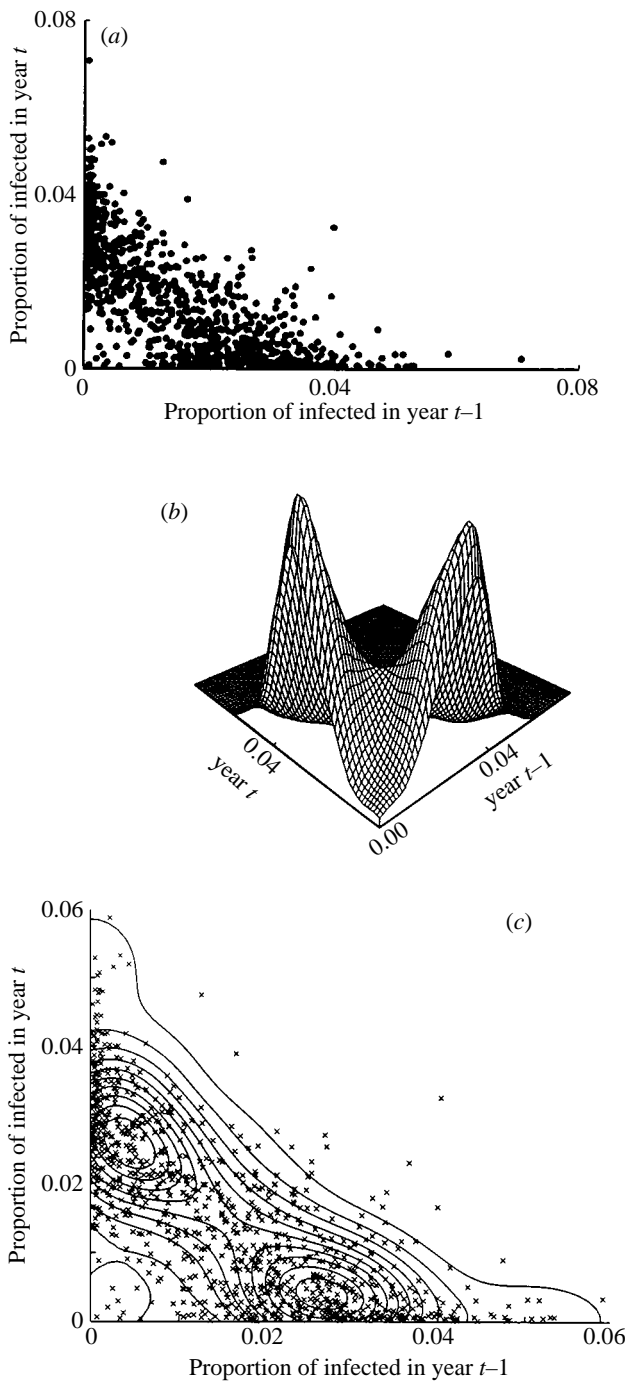


Figure 2. Real data, pre-vaccination 1948–1966. (a) Scatterplot of  $c_{i,t}$  against  $c_{i,t-1}$ . (b) Joint density of scatterpoints. (c) Contour lines of estimated joint density, for observed data ( $i = 1, \dots, 60$ ) during the pre-vaccine era (960 data points). The scatterpoints superimposed on the contour lines in (c) are model data for a median-sized population with mean birth rate.

product kernel. As a starting point, we used the normal referencing bandwidth given by Silverman (1986), i.e.

$$\text{bandwidth} = 1.06s_c n^{-\frac{1}{6}},$$

where  $n$  is the number of observations, and  $s_c$  is the estimated standard deviation of  $c_{i,t}$ . However, since it is based on the normal distribution, the Silverman rule is oversmoothing. We deliberately corrected for this by using 0.7 times the bandwidth, which reveals additional information about modes

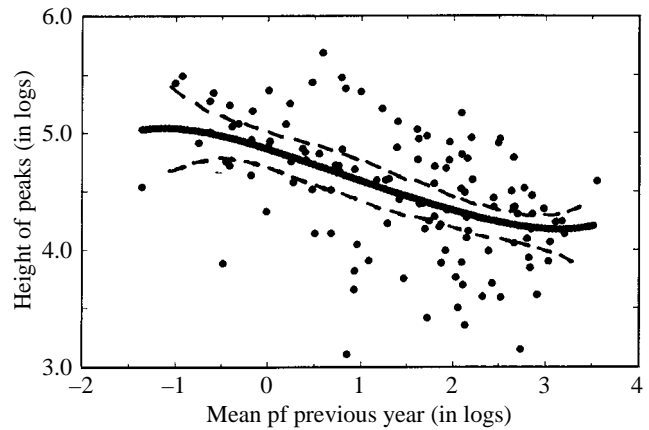


Figure 3. Maximum height of peak versus mean of previous minor epidemic year on natural log scale for the 12 largest cities in the sample set. Data standardized by population size. The solid line denotes the estimated smooth relationship (Gaussian kernel, normal referencing bandwidth (Silverman 1986)). The dashed lines are 95% percentiles of the nonparametric estimation applied to 300 replications of pairwise bootstrap drawings of the same sample size. The estimated rank correlation coefficient is  $-0.53$ .

becoming unstable. However, we also checked that the results reported below do not vary for a wide range of smoothing parameters, including the normal referencing bandwidth given above.

3. The contour lines corresponding to the joint density.

### 3. RESULTS

#### (a) *Basic patterns in the observed data before vaccination*

To clarify which interesting dynamical features can be extracted from the joint density, let us consider the form of the three plots for the entire pre-vaccination data set (figure 2). The most striking feature is that they reveal a *negative density dependence* between successive major and minor epidemics: this means that the overall number of cases during a two-year wave approximately ‘consumes’ a fixed proportion of the population (Finkenstädt & Grenfell 1998). Secondly, the plots reveal information about the underlying *cyclicity*. The clustering in figure 2a indicates the predominance of the biennial pattern where the major epidemic years are regularly followed by minor epidemic years and vice versa. This implies that the joint density in figure 2b has *two modes* which are most frequently visited. Thirdly, the plots provide an insight into the *regularity* of the data. If the underlying cyclicity is irregular in the sense that main epidemics are occasionally missed out then (a) the density-dependent negative relationship will be more dispersed and (b) there will be a higher density of scatterpoints near the origin. Figure 2c shows the contours of the estimated joint density. The points imposed on the contours are for model data for a medium-sized city (200 000 inhabitants) with a birth rate equal to the mean observed birth rate (0.017 per person per year). Figure 2c demonstrates that real and model data are compatible with respect to both their range and

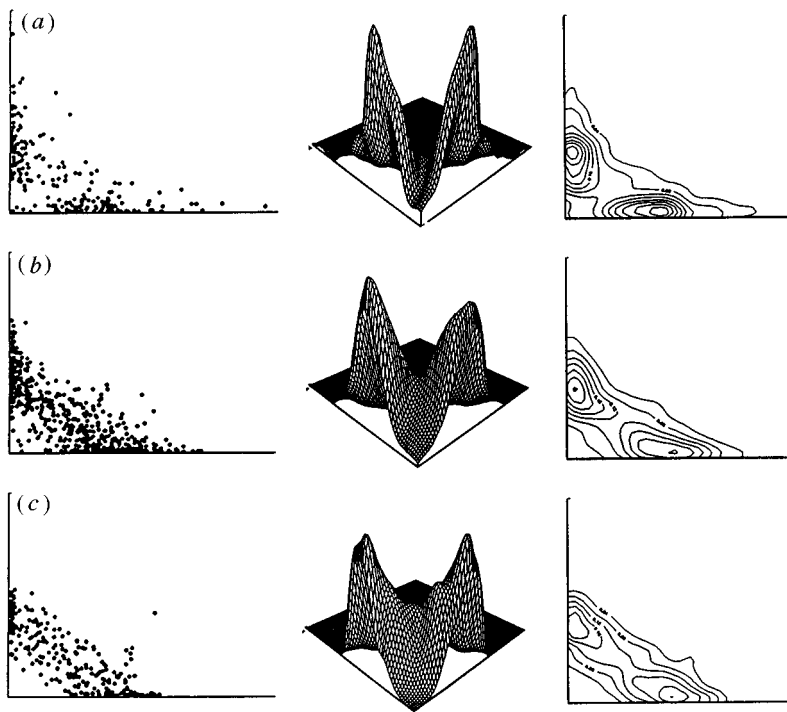


Figure 4. Set of plots (scatterplot, joint density, contour lines) for observed pre-vaccination data. The data are pooled into three different population size classes: (a)  $< 100\,000$ ; (b)  $100\,000 - 250\,000$ ; (c)  $> 250\,000$ . The number of data points are 208, 518, 234 for the low, medium and high population level.

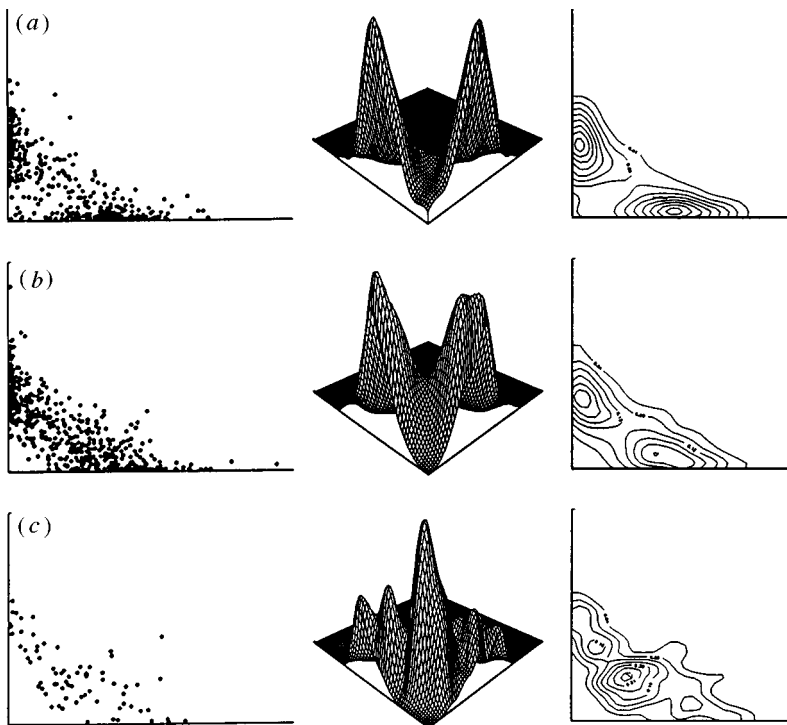


Figure 5. Set of plots (scatterplot, joint density, contour lines) for observed pre-vaccination data where the data are pooled into three different birth rate classes: (a)  $< 0.016$ ; (b)  $0.016 - 0.02$ ; (c)  $> 0.02$ . The number of data points are 372, 518, 70 for the low, medium and high birth rate levels.

cyclicly. The two biennial modes are also clearly visible in both model and data.

Figure 2 reflects two processes: the biennial epidemic pattern and the negative density dependence between successive years. Figure 3 focuses on the latter by explicitly estimating the relationship between the major peak height and the mean of the previous minor epidemic year for the 12 largest centres. The nonparametric curve indicates the negative decline in that low troughs are followed by high peaks and vice versa (Spearman rank correlation

$= -0.53$ ). This clearly illustrates the negative density dependence embedded in figure 2. This pattern is also present—although it is more noisy—in smaller centres.

To summarize, the smooth joint density enables us to extract information regarding important characteristics of the underlying attractor such as cyclicly, regularity, and negative density dependence. We now explore how these characteristics change with respect to (1) spatial variations in population size and (2) spatiotemporal variations in birth rate.

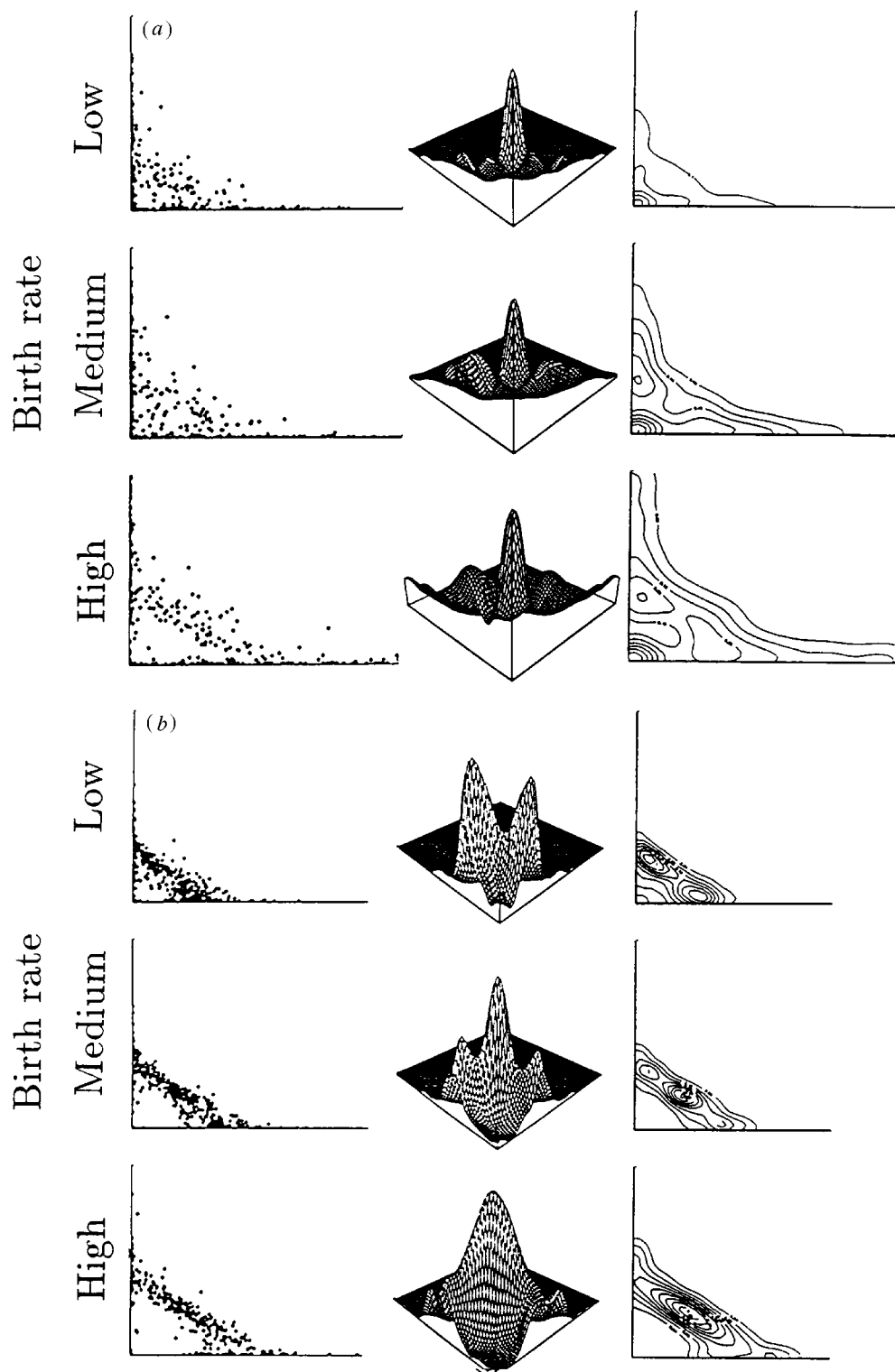


Figure 6. Set of plots (scatterplot, joint density, contour lines) for simulated data from realistic age-structured compartment (PRAS) model for three different population sizes, (a) 20 000; (b) 200 000; (c) 2 million, and three birth rate levels (rows). Each group contains 300 data points.

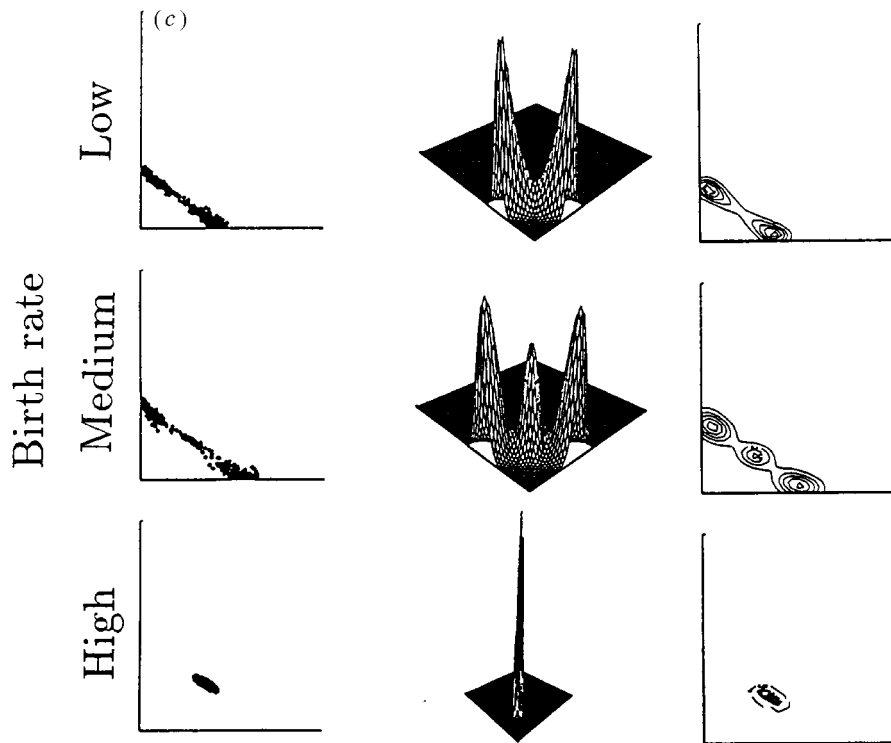


Figure 6. (Cont.)

**(b) Effect of variations in demographic parameters**

(i) Pre-vaccination era

Observed data

*Variations in population size.* Figure 4 shows the joint density and the corresponding plots where the data are pooled into three classes of population size: small towns with less than 100 000 inhabitants (13 towns), medium towns with 100 000–250 000 inhabitants (32 towns), and large communities above the CCS (15 towns).

For each class, the joint density is bimodal, indicating that the biennial cycle predominates irrespective of the local population size. However, the regularity of the relationship and the negative density dependence do vary with population size. Figure 4 shows that the height of the joint density between the two biennial modes rises with population size. For large communities, the relationship between the major and minor epidemic years implies relatively low major epidemics in conjunction with a higher proportion of cases during the minor epidemics. The relationship between  $c_{i,t}$  and  $c_{i,t+1}$  is monotonic and less dispersed for the large centres than for the small ones. For the latter, it is difficult to predict the magnitude of the following major epidemic, in particular if the previous minor epidemic has been small. The clustering of scatterpoints towards the origin indicates a lack of regularity, in that smaller places sometimes miss out on main epidemics (Cliff *et al.* 1993).

The sequence of plots in figure 4 therefore summarizes the transition from the sporadic pattern of the disease in small places (type III dynamics) to the smooth, regular endemic pattern of the large centres (type I and II dynamics) as classified by Bartlett (1957).

*Variations in birth rate.* In figure 5, the data are pooled into three different classes according to the four year delayed

birth rate: low birth rate (less than 0.016 per person per year), medium birth rate (between 0.016 and 0.02) and high birth rate (larger than 0.02). Since birth rate was subject to more temporal variations than population size, the data for one city are not necessarily pooled into the same class. Because birth rate peaked in 1947, the high birth rate class mainly contains data points from the early 1950s. Some cities, such as Liverpool, Sunderland, and Coventry, are in the highest birth rate class almost throughout the whole study period. The distinctive shape of the dynamics of communities with high birth rates is also addressed by Grenfell *et al.* (1994a) and Finkenstädt & Grenfell (1998).

For low birth rates, the two-year cyclicity is clearly predominant. However, the two modes gradually merge towards one mode in the high birth rate class, where annual cyclicity becomes predominant. This observation is supported by our previous study (Finkenstädt & Grenfell 1998), where it was shown that the birth rate has an increasing effect in particular on the minor epidemic years due to a quicker replacement of susceptibles after major epidemics (Grenfell *et al.* 1994a,b, 1995a). The impact of the minor epidemic de-emphasizes the biennial pattern towards a predominant annual pattern. Most interestingly, figure 5 illustrates the empirical analogue of a period doubling bifurcation (May 1976) for decreasing values of the birth rate parameter.

Model data

Figure 6 summarizes the transitions of the model time-series for three levels of population size (20 000, 200 000, 2 million) and three levels of birth rate (0.015, 0.019, 0.024) along the vertical axis. These values fall within the low, medium, and high categories taken for the real data, so that parameter values are comparable.

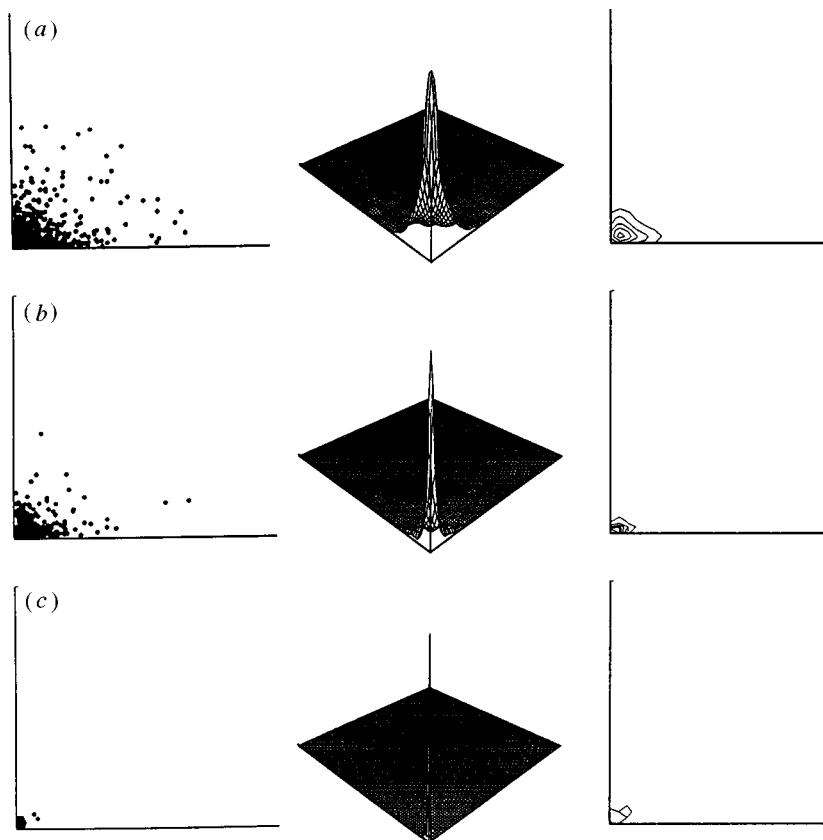


Figure 7. Sequence of plots (scatterplot, joint density, contour lines) for observed post-vaccination data. Data are pooled into three classes of successive time-periods after vaccination was taken up: (a) 1972–1982; (b) 1982–1992; (c) 1992–1994. The number of data points are 600, 480, 120 for the subsequent time-spans.

Consider the changes in pattern for varying demographic parameters. The small populations (figure 6a) generally behave irregularly with a high frequency of points close to the origin. For increasing birth rate, the joint density bifurcates from a single mode close to the origin towards a bimodal pattern. The corresponding dynamics therefore evolves from irregular behaviour with sporadic outbreaks of infection towards a state where biennial cycles become frequent. The large and medium-sized populations (figure 6b,c) exhibit regular two-year cycles at low birth rates which become unstable and merge towards annual cyclicity for high birth rates. Increasing the population size causes a transition from irregular behaviour towards regular endemic cycles, which may be biennial or annual (or a mixture) depending on the level of the birth rate. The negative density dependence therefore progresses from the dispersed, least predictable relationship for small places towards a predictable, smooth relationship for large towns.

Figure 6 shows that both parameters, population size and birth rate, act as bifurcation parameters on the joint density, displaying a single mode at the extremes of a small population with a low birth rate or a large population with a high birth rate. Elsewhere, two modes, and hence biennial dynamics, dominate.

(ii) *Post-vaccination era*

Figure 7 shows the delay plots for successive periods after the onset of the vaccination programme. Since vaccination modulates the recruitment rate of susceptibles from births, but detailed information on the spatial variations in vaccine uptake is not available, we cannot disentangle the

impact of birth rate variations during the vaccine era. As predicted by theory (Anderson & May 1991), figure 7 reveals a reduction in the tendency for biennial epidemics. Graphs (a)–(c) show that the overall incidence pattern declines with the trend of increasing vaccine uptake in time. There is effectively no visible pattern other than the secular decline in disease incidence.

#### 4. DISCUSSION

Both data and models indicate a strong density-dependent signature in the sequence of pre-vaccination measles epidemics in England and Wales. More generally, the results illustrate that the joint density summarizes useful information about the behaviour of ecological time-series around the deterministic attractor. Using the annual number of measles cases in 60 communities in England and Wales, the joint density has been shown to be affected by demographic parameters such as population size and birth rate. From the joint density, we can infer the dynamics of the local population, and these results agree well with intuition. Small populations suffer from irregular dynamics and long fadeouts, whereas the dynamics of large populations lies closer to the attractor. Moreover, both models and data exhibit very similar dynamical patterns. Specifically:

1. the model predicts proportions of cases that approximately lie in the same range as the real data.
2. there is a negative density dependence between successive minor and major epidemics, the predictability of which improves with a larger population size. The

dynamical behaviour evolves from an irregular occurrence of the disease in the small places towards a regular endemic pattern for large communities.

- for medium and larger cities the model predicts a transition from biennial towards annual cyclicity for an increasing birth rate. Figure 6 shows the empirical analogue of such bifurcation in the real data.

It is reassuring to find that the model—which represents the global attractor—also has similar behaviour to the real system far from the stable orbit, and for small populations when the level of stochasticity is relatively large.

Both models and observed data show that the transition from biennial to annual epidemics in large populations is driven by an increasing birth rate. This is a particularly clear example of a change in dynamic behaviour driven by a population parameter. More generally, our results parallel recent work on the dynamical effect of spatial (Bjørnstad *et al.* 1995; Stenseth *et al.* 1996b) and temporal (Dennis *et al.* 1995; Costantino *et al.* 1995, 1997) parameter variations in ecological systems. There is a particular analogy with the *Tribolium* work (Costantino *et al.* 1997), since these researchers find a simplification of system dynamics with decreasing mortality rate of adult beetles, which is broadly analogous with the effects of increasing birth rates on measles epidemics. However, we also see *spatial* variations in measles dynamics, because of the spatio-temporal pattern of birth rate heterogeneities.

Measles is also unusual because it allows us to test how the dynamic effects of parameter shifts interact with demographic stochasticity. In small towns, where demographic noise is relatively high, we see a dynamic transition with increasing birth rate from irregular outbreaks to more biennial patterns. By contrast, the equivalent transition in large centres—which are much more buffered against demographic noise—is from biennial to annual epidemics. The pattern in large centres is the one we would predict from simple deterministic models (McLean & Anderson 1988a,b). In small centres, this picture is complicated by local extinctions of infection, which can lead to *successive* years without major epidemics, if the birth rate is low (the points near the origin in graph (a) of figure 5). Further modelling and time-series analysis of epidemics in small centres is required to clarify these interesting patterns completely.

Finally, what does this analysis tell us about the long-term stability of the measles attractor? Before vaccination, there is clear evidence of a density-dependent tendency to return to the biennial limit cycle. Classical models of unforced measles dynamics (Anderson & May 1991) predict that this tendency is weak—epidemics damp very slowly to the deterministic attractor. This is also the case for the nonlinearities documented here. For the vaccine era, the basically biennial epidemic pattern seen before vaccination gives way to irregular epidemics of low amplitude (Aron 1990; Ferguson *et al.* 1996). The resulting signature of density dependence is much less clear than that for the pre-vaccination era. Apart from the reduction in cases and the amplitude of epidemics, the most dramatic impact of vaccination has been a statistical decorrelation of epidemics (Bolker & Grenfell 1995). Teasing out whether this arises from a reduction in density-dependent

feedbacks—as documented here—or other dynamic effects is an important area for future research.

This work was supported by the Wellcome Trust (B.F., M.K. and B.G.) and the Royal Society (B.G.). We would like to thank the referees for helpful comments.

## REFERENCES

- Anderson, R. M. & May, R. M. 1991 *Infectious diseases of humans: dynamics and control*. Oxford University Press.
- Aron, J. L. 1990 Multiple attractors in the response to a vaccination program. *Theor. Popul. Biol.* **38**, 58–67.
- Bartlett, M. S. 1956 Deterministic and stochastic models for recurrent epidemics. In *Proc. Third Berkeley Symp. Math. Stats. Prob.* **4**, 81–108.
- Bartlett, M. S. 1957 Measles periodicity and community size. *J. R. Statist. Soc. A* **120**, 48–70.
- Bartlett, M. S. 1960 The critical community size for measles in the US. *J. R. Statist. Soc. A* **123**, 37–44.
- Bjørnstad, O. N., Falck, W. & Stenseth, N. C. 1995 Geographic gradient in small rodent density fluctuations—a statistical modelling approach. *Proc. R. Soc. Lond. B* **262**, 127–133.
- Bjørnstad, O. N., Champely, S., Stenseth, N. C. & Saitoh, T. 1996 Cyclicity and stability of grey-sided voles, *Clethrionomys rufocanus*, of Hokkaido—spectral and principal components analyses. *Phil. Trans. R. Soc. Lond. B* **351**, 867–875.
- Bolker, B. M. & Grenfell, B. T. 1995 Space, persistence and the dynamics of measles epidemics. *Phil. Trans. R. Soc. Lond. B* **348**, 309–320.
- Clarkson, J. A. & Fine, P. E. M. 1985 The efficiency of measles and pertussis notification in England and Wales. *Int. J. Epidemiology*, **14**, 153–168.
- Cliff, A. D., Haggett, P. & Smallman-Raynor, M. 1993 *Measles: an historical geography of a major human viral disease from global expansion to local retreat, 1840–1990*. Oxford: Blackwell.
- Costantino, R. F., Cushing, J. M., Dennis, B. & Desharnais, R. A. 1995 Experimentally induced transitions in the dynamic behaviour of insect populations. *Nature* **375**, 227–230.
- Costantino, R. F., Desharnais, R. A., Cushing, J. M. & Dennis, B. 1997 Chaotic dynamics in an insect population. *Science* **275**, 389–391.
- Dennis, B., Desharnais, R. A., Cushing, J. M. & Costantino, R. F. 1995 Non-linear demographic dynamics, mathematical models, statistical methods, and biological experiments. *Ecol. Monogr.* **65**, 261–281.
- Dietz, K. & Schenzle, D. 1985 Mathematical models for infectious disease statistics. In *A celebration of statistics* (ed. A. C. Atkinson & S. E. Feinberg), 167–204. New York: Springer.
- Ferguson, N. M., Nokes, D. J. & Anderson, R. M. 1996 Dynamical complexity in age structured models of the measles virus: epidemiological implications at high levels of vaccine uptake. *Mathematical Biosci.* **183**, 101–130.
- Finkenstädt, B. & Grenfell, B. T. 1998 Empirical determinants of measles metapopulation dynamics in England and Wales. *Proc. R. Soc. Lond. B* **265**, 211–220.
- Framstad, E., Stenseth, N. C., Bjørnstad, O. N. & Falck, W. 1997 Limit cycles in Norwegian lemmings: tensions between phase-dependence and density-dependence. *Proc. R. Soc. Lond. B* **264**, 31–38.
- Gilpin, M. & Hanski, I. 1991 *Metapopulation dynamics: empirical and theoretical investigations*. London: Academic Press.
- Grenfell, B. T. 1992 Chance and chaos in measles dynamics. *J. R. Statist. Soc. B* **54**, 383–398.
- Grenfell, B. T., Kleczkowski, A., Ellner, S. P. & Bolker, B. 1994a Non-linear forecasting and chaos in ecology and epidemiology: measles as a case study. In *Chaos and forecasting* (ed. H. Tong), pp. 321–345. Singapore: World Scientific.

- Grenfell, B. T., Kleczkowski, A., Ellner, S. P. & Bolker, B. M. 1994b Measles as a case-study in nonlinear forecasting and chaos. *Phil. Trans. R. Soc. Lond. A* **348**, 515–530.
- Grenfell, B. T., Bolker, B. M. & Kleczkowski, A. 1995a Demography, seasonality and the dynamics of measles in developed countries. In *Epidemic models: their structure and relation to data* (ed. D. Mollison), pp. 248–270. Cambridge University Press.
- Grenfell, B. T., Bolker, B. M. & Kleczkowski, A. 1995b Seasonality and extinction in chaotic metapopulations. *Proc. R. Soc. Lond. B* **259**, 97–103.
- Grenfell, B. T. & Harwood, J. 1997 (Meta)population dynamics of infectious diseases. *Trends Ecol. Evol.* **12**, 395–399.
- Higgins, K., Hastings, A., Sarvela, J. N. & Botsford, L. W. 1997 Stochastic dynamics and deterministic skeletons: population behaviour of Dungeness crab. *Science* **276**, 1431–1435.
- Hill, J. K., Thomas, C. D. & Lewis, O. T. 1996 Effects of habitat patch size and isolation on dispersal by *Hesperia comma* butterflies: implications for metapopulation structure. *J. Anim. Ecol.* **65**, 725–735.
- Keeling, M. J. & Grenfell, B. T. 1997 Disease extinction and community size: modeling the persistence of measles. *Science* **275**, 65–67.
- Keeling, M. J. & Grenfell, B. T. 1998 Infectious imports, spatial heterogeneity and vaccination in measles models. (In preparation.)
- Mclean, A. R. & Anderson, R. M. 1988a Measles in developing countries. Part I. Epidemiological parameters and patterns. *Epidemiology Infect.* **100**, 111–133.
- Mclean, A. R. & Anderson, R. M. 1988b Measles in developing countries. Part II. The predicted impact of mass vaccination. *Epidemiology Infect.* **100**, 419–442.
- May, R. M. 1976 Simple mathematical models with very complicated dynamics. *Nature* **261**, 459–467.
- May, R. M. 1982 *Theoretical ecology: principles and applications*. Oxford: Blackwell.
- Nee, S. 1994 How populations persist. *Nature* **367**, 123–124.
- Olsen, L. F., Truty, G. L. & Schaffer, W. M. 1988 Oscillations and chaos in epidemics: a nonlinear dynamic study of six childhood diseases in Copenhagen, Denmark. *Theor. Popul. Biol.* **33**, 344–370.
- Rand, D. A. & Wilson, H. B. 1991 Chaotic stochasticity: a ubiquitous source of unpredictability in epidemics. *Proc. R. Soc. Lond. B* **246**, 179–142.
- Ranta, E., Kaitala, V., Lindstrom, J. & Helle, E. 1997 The Moran effect and synchrony in population dynamics. *Oikos* **78**, 136–142.
- Rhodes, C. J., Jensen, H. J. & Anderson, R. M. 1997 On the critical behaviour of simple epidemics. *Proc. R. Soc. Lond. B* **264**, 1639–1646.
- Royama, T. 1992 *Analytical population dynamics*. London: Chapman & Hall.
- Saitoh, T., Stenseth, N. C. & Bjørnstad, O. N. 1997 Density dependence in fluctuating grey-sided vole populations. *J. Anim. Ecol.* **66**, 14–24.
- Schaffer, W. M. & Kot, M. 1985 Nearly one-dimensional dynamics in an epidemic. *Theor. Biol.* **112**, 403–427.
- Schenzle, D. 1984 An age-structured model of pre- and post-vaccination measles transmission. *IMA J. Mathematics Appl. Med. Biol.* **1**, 169–191.
- Silverman, B. W. 1996 *Density estimation*. London: Chapman & Hall.
- Stenseth, N. C., Bjørnstad, O. N. & Falck, W. 1996a Is spacing-behaviour coupled with predation causing the microtine density cycle? A synthesis of current process-oriented and pattern-oriented studies. *Proc. R. Soc. Lond. B* **263**, 1423–1435.
- Stenseth, N. C., Bjørnstad, O. N. & Saitoh, T. 1996b A gradient from stable to cyclic populations of *Clethrionomys rufocanus* in Hokkaido, Japan. *Proc. R. Soc. Lond. B* **263**, 1117–1126.
- Sutcliffe, O. L., Thomas, C. D. & Moss, D. 1996 Spatial synchrony and asynchrony in butterfly population dynamics. *J. Anim. Ecol.* **65**, 85–95.
- Sutcliffe, O. L., Thomas, C. D., Yates, T. J. & Greatorex-Davies, J. N. 1997 Correlated extinctions, colonizations and population fluctuations in a highly connected ringlet butterfly metapopulation. *Oecologia* **109**, 235–241.

As this paper exceeds the maximum length normally permitted, the authors have agreed to contribute towards production costs.